Click to see Slides of Oral Presentation

The Cutoff of Flowing Porosity in Tight Complex Carbonate Oil Reservoir: A Case Study on High-Pressure Mercury Intrusion in Interval MBK, Block SH, Iraq*

Yaping Lin[1], Tiezhuang Wu[1], Chaosheng Guo[2], Liyong Tan[3], Xiaofeng Sheng[1], and Chuandi Wang[4]

Search and Discovery Article #42204 (2018)**
Posted April 30, 2018

*Adapted from extended abstract based on oral presentation given at GEO 2018 13th Middle East Geosciences Conference and Exhibition March 5-8, 2018, Manama, Bahrain

[1]RIPED, Beijing, China (llinyaping-hw@petrochina.com.cn)
[2]Bureau of geophysical prospecting, Zhuozhou, China
[3]Greatwall drilling company, Beijing, China
[4]CNOOC, Beijing, China

Abstract

Based on the porosity measured by high pressure mercury intrusion and helium experiments, and analysis of oil saturation data of 29 samples of tight formations of interval MBK in SH block, in the northwest of Kurdish Region of Iraq, the cutoff value of flowing porosity in tight complex carbonate oil and its controlling factors are determined. According to the conversion between capillary pressure in reservoir conditions and capillary pressure from high pressure mercury intrusion experiments, flowing porosity in various injection pressures in reservoir condition can be calculated. By calculating the minimum flowing porosity of oil-bearing samples and the maximum flowing porosity of the samples without oil, it is confirmed that 3.1% is the lowest limit for the flowing porosity in oil-bearing samples in the study area; and the corresponding injection pressure in reservoir conditions is 19.9 Psi. If the injection pressure is higher than 19.9 Psi, the oil can freely flow and accumulate.

The relationships among flowing porosity, injection pressure, and pore-throat-ratio are shown by the analysis of pore-throat-ratio, injection pressure, and the 4 different reservoir types (the fracture porosity type, the porosity one, the vuggy one, and the complex one). The flowing porosity of tight carbonate formations and pore-throat-ratio are negatively related. The poorer connectivity of pore-throat in reservoirs is, the higher injection pressure is needed for the flowing porosity to be 3.1%. The injection pressure has a negative correlation to reservoir quality index (RQI). With the reservoir quality index (RQI) increasing, the injection pressure, which is needed for flowing porosity to be 3.1%, is in a decreasing tendency. On the basis of the cutoff value of tight complex carbonate of the flowing porosity and injection pressure in reservoir conditions, the discriminant chart of effective accumulation of tight oil in complex carbonate is established.

Background

The block SH is located approximately 80 km northwest of Erbil, in the northern Kurdistan region of Iraq. It is situated in the foothills of the Zagros Mountains (Taurus Trend), where the terrains begin to be flatten to the south into the Mesopotamian Basin. The Zagros foreland basin includes nappe zones and simple fold zones. The carbonate reservoirs in the basin are extremely rich in oil and gas resources, to which more than 30 oil fields bear witness. The anticlines in this area are formed by the compression of the Zagros orogenic belt. The long axis anticlines are widely distributed and parallel to the orogenic belt. The oil and gas fields are discovered in almost all the long axis anticlines here, shown in Figure 1.

Introduction

For the study of the cutoff of carbonate reservoir, there are some subjective factors in the traditional methods (such as: oil testing, experience, normal and inverse cross-plot method, etc.), and also it lacks analysis of main controlling factors and theoretical demonstration. In this study, the authors clarify kinds of parameters and porosities, combine porosity model with high-pressure mercury intrusion experiments, and then determine the porosity cutoff of the reservoir.

Total porosity refers to the ratio of the total volume of all the pores to the total volume of the rock, and it can generally be obtained by the weighing method. Effective porosity is the ratio of the interconnected pore volume to the total volume of the rock under a certain pressure that can be obtained by gas-measurement. Flowing porosity is the ratio of movable volume to the total rock volume in a saturated rock sample at a given pressure, it can be obtained by high-pressure mercury intrusion.

High-pressure mercury injection can be used to characterize the capillary pressure in tight reservoirs (Lucia, 2007; Zhang et al., 2014; Gong et al., 2015) effectively and to establish the relationship between the saturation of minimum wetness and pressure, so as to characterize the parameters of movable fluid effectively. Therefore, the experiment can be used to calculate the flowing porosity accurately under different mercury pressures. In this article, the flowing porosity characteristics of tight carbonate reservoirs were studied, the low limit and the controlling factors of flowing porosity of interval MBK in this block were determined.

Method and Results of High-Pressure Experiment

Experiment Method

The SH block develops tight carbonate in the MBK Formation, where industrial oil flow was discovered. Samples of wells S-1 and S-6 were selected for this study. Both S-1 and S-6 were well cored in the MBK. System coring was performed on the oil-bearing carbonate reservoirs. A total of 29 samples from interval MBK were selected for high-pressure mercury intrusion experiment.

The experiment device for high-pressure mercury intrusion, called PoreMaster GT60, was used; and the experiment steps were based on China national standards which was named GB/T_21650.1-2008. The experiment conditions were as following: laboratory temperature ranged from

22℃ to 25℃, mercury surface tension was 480 mN/m, mercury contact angle was 140°, dilatometer volume was 0.5 ml, and the equipment pressure range was 10-65,000 Psi. The maximum mercury pressure ranges mainly from 1584 Psi to 59,976 Psi in this actual measurement.

Experiment Results

According to the observation of carbonate rock samples and the mercury intrusion experiment analysis, the 29 samples can be divided into the following four categories: the fracture porosity type, the porosity one, the vuggy one and the complex one. In this experiment, the helium-measured porosity of 29 samples ranges from 0.7% to 10.1%, the mercury-measured porosity is in the range of 0.5%-7.0%, and the air permeability ranges from 0.001 mD to 1.612 mD. Based on the definition of the porosity model, the He-measured porosity of the samples is the effective porosity, the porosity measured by the high-pressure mercury intrusion experiment is the flowing porosity. The flowing porosity should be less than the effective porosity (Hong, 2014), and it is well proven by the two groups of the porosity (shown in Table 1), the main reason for the difference is the effect of mercury and He-gas on the rock interface.

The mercury-measured porosity has a positive relationship with conformance volume (Figure 3). The conformance volume increases from 0.00001 cm^3/g to 0.00580 cm^3/g, meanwhile the mercury-measured porosity increases from 0.5% to 7.0%. The differences of maximum mercury pressure of different samples are obvious, the minimum is 1584 Psi, the maximum is 59,976 Psi. The maximum mercury injection pressure is nonlinearly negatively correlated with the average pore radius of the reservoir (Figure 4). The smaller the average reservoir pore radius is, the greater the maximum mercury injection pressure is. When the average pore radius of reservoir is less than 0.01um, the maximum mercury intrusion pressure is over 40,000 Psi. When the average pore radius of reservoir ranges from 0.01 um to 0.2 um, the maximum mercury intrusion pressure ranges from 7000 Psi to 15,000 Psi. When the average pore radius of reservoir is more than 0.2 um, the maximum mercury pressure is generally less than 4000 Psi.

Analysis and Discussion

Experiment Mercury Injection Pressure and the Injection Pressure Under Reservoir Conditions

In the high-pressure mercury injection experiment (Li et al., 2013), the measured mercury injection pressure is converted into a capillary pressure which is different from the capillary pressure under reservoir conditions. In this study, it is assumed that the pore throat radius is not changed here. So, the capillary pressure obtained from the high-pressure mercury intrusion experiment can be converted into the capillary pressure under reservoir conditions. The sample depth ranges from 2249 m to 2307 m, the average geothermal gradient of 2.0℃/100 m with a surface temperature of 31℃, the average reservoir temperature is about 78℃, the pressure coefficient is about 1.053~1.160, the formation pressure ranges from 24 MPa~27 MPa. Under the corresponding temperature and pressure conditions, the interface tension between oil and brine water is 25 mN/m and the wetting angle between water and rock is 0. The mercury surface tension is 480 mN/m, the wetting angle is 140°. According to capillary pressure formula:

$$Pc = 2\sigma\cos\theta\ r \qquad (1)$$

$$Pco = \sigma o\ \cos\theta o\ \sigma Hg\ \cos\theta Hg \times PcHg \qquad (2)$$

$$Pco = 0.07 \times PcHg \qquad (3)$$

Based on equation (3), we can get the injection pressure under different reservoir conditions with different mercury intrusion pressures. The initial mercury injection pressure of the samples in the block distributed between 62.8 Psi and 6644.4 Psi, and the injection pressure under reservoir conditions was calculated to be 4.4 Psi to 465.1 Psi.

The Cutoff of Flowing Porosity Under Reservoir Conditions

For the all samples here, the experiment results show that the flowing porosity of sample No. S74 in carbonate reservoir MBK under the maximum mercury intrusion pressure is 3.8% and the effective porosity is 4.7%. The flowing porosity of sample No. S56 under the maximum mercury intrusion pressure is 4.2% and the effective porosity is 4.4%, but the oil saturation is 58.7% by the extraction method (Li et al., 2013; Hong et al., 2014). And also the three core samples (S65, S79 and S39) from Well S-1 and Well S-6 demonstrate oil show from no to good (Figure 5). Therefore, although the low limit of effective porosity is set as 4.5% for the calculation of reserves by predecessors, the low limit of effective porosity should be less than 4.5%. Since sample S74 was not measured for oil saturation, only some oil show in the core was observed, the 3.8% was chosen as the minimum of flowing porosity for the oil-bearing samples. The average difference between the flowing porosity and the effective porosity of the samples is 1.20%.

Although oil saturation measurements were not performed in samples with no oil show, the analysis of core and mud log can illustrate the oil show situation. Unlike the samples with oil show, the maximum flowing porosity of oil-free samples is 3.8%, the average value is 2.5%. The maximum effective porosity of oil-free samples is 6.1%, and the average value is 3.3%. So, the average difference between the flowing porosity and the effective porosity of samples with no oil is 0.8%.

Based on the mercury injection research, if the throat radius (Hong et al., 2014; Gong et al., 2015) is less than 0.015 um (Figure 6a) in this area, the Max Hg press increases sharply, as a result, the cutoff of this radius is given to be 0.015um. The distribution of flowing porosity is illuminated by histogram plots, and the low limit value is obtained by using the normal and inverse cross-plot (Figure 6b), which is determined to be 3.1%.

It should be noted that the cutoff of the flowing porosity can be changed in different areas, which is greatly influenced by the source rock thickness, hydrocarbon generation intensity and the fractures (micro-fractures). The cutoff values vary greatly in different areas, but it should be a given value here.

Flowing Porosity Under Reservoir Conditions with Different Injection Pressures

When the flowing porosity is less than 3.1%, the crude oil cannot flow effectively. The flowing porosity of most samples with no oil do not reach the low limit in the study (shown in Table 1), while the flowing porosity of oil-bearing samples is greater than 3.1%. Therefore, this study takes samples with oil as an example to discuss the relationship between injection pressure and flowing porosity under reservoir conditions (Lucia, 2007; Hu et al., 2012; Harbaugh, 1967).

From formula (3), the flowing porosity under different pressures injection can be obtained from the high-pressure mercury intrusion experiment. The 17 oil-bearing samples of MBK were analyzed. Five sets of experiment data were selected and the mercury intrusion pressures were 143 Psi, 429 Psi, 715 Psi, 1430 Psi and 2860 Psi. The calculated injection pressures by formula (3) under reservoir conditions were 10 Psi, 30 Psi, 50 Psi, 100 Psi and 200 Psi. When the injection pressure was 10 Psi and the reservoir flowing porosity of the 11 samples was between 0.8% and 2.3%, the fluidity of reservoir was good, while the flowing porosity of the other 6 samples (S14, S54, S56, S62, S67 and S74) was less than 1.5%, the reservoir fluidity was weak.

When the injection pressure increased from 10 Psi to 30 Psi, the fluidity of most samples changed. The flowing porosity of the 11 samples increased from 47.2% to 71.6% of the maximum, the flowing porosity of most samples was greater than the cutoff, and therefore, the crude oil in this interval can be effectively aggregated. However, the flowing porosity of the other 6 samples (S14, S54, S56, S62, S67 and S74) was increased from less than 1.8% to 1.6%-2.6%, and reservoir fluidity was still limited (Table 2).

When the injection pressure increased from 30 Psi to 50 Psi, to 100 Psi. The fluidity of the 17 oil-bearing samples of increased obviously, the flowing porosity reached 81%-95% of the maximum porosity at 100 Psi injection pressure, the average flowing porosity was about 4.8%, which was greater than the low limit in this block. When the injection pressure increased from 100 Psi to 200 Psi, although the flowing porosity of the oil-bearing samples increased slowly, the average flowing porosity still increased from 4.8% to 5.2%, showing that the fluidity of samples increased again, and the flowing porosity reached 92%-98% of the maximum. When the injection pressure increased from 200 Psi to the maximum injection pressure, the flowing porosity of most samples changed little.

When the flowing porosity was up to 3.1%, the injection pressures under the reservoir conditions of most samples in formation MBK were less than 30 Psi and the average was 19.9 Psi, except the pressures of those samples such as S14, S56, S62 and S67, were over 40 Psi. It indicated that the tight oil in this compact carbonate reservoir can agglomerate and flow effectively at a reservoir pressure of 19.9 Psi.

Controlling Factors of Flowing Porosity

Flowing porosity can characterize the fluidity of reservoirs. It is of great significance to hydrocarbon accumulation in the tight carbonate reservoirs with different injection pressures under reservoir conditions. In addition to being controlled by reservoir pressure, flowing porosity is controlled by the reservoir micro-structure. Three important characterization parameters (pore-throat ratio (Lucia, 2007; Rockwood et al., 1957; Rafatian et al., 2015; Anderson, 1987; Feng et al., 2012), reservoir quality index (RQI) and the ratio of minimum pore-throat radius and 50% probability of pore-throat radius (RMP)) were selected to fit with the flowing porosity (shown in Figure 7a, b, c).

The fitting results show that when the pore-throat ratio is less than 2, there is no obvious relationship between the flowing porosity and the pore-throat ratio. It indicates that when the reservoir connectivity is good, the flowing porosity is mainly controlled by the injection pressure and other reservoir factors. When the pore-throat ratio is greater than 2, the flowing porosity is negatively correlated with the pore-throat ratio (Figure 7a). At this time, the reservoir pore throat connectivity is poor, and the pore-throat ratio plays an important role in controlling flowing porosity.

When the reservoir quality index (RQI) is less than 0.8, the relationship between flowing porosity and RQI is in a mass; when the RQI is greater than 0.8, the flowing porosity is positively correlated with the RQI, but the correlation is weak (Figure 7b). The relationship between RMP and flowing porosity is negative, when RMP increases, the flowing porosity is in a decrease trend (Figure 7c). When the flowing porosity reaches 3.1%, the injection pressure shows a significant positive correlation with the pore-throat ratio (Figure 8a, b), it shows that the reservoir pore-throat connectivity deteriorates, requiring a higher pressure for flowing porosity of 3.1%. The increase of pore-throat ratio will affect the micro fluidity of reservoir. The injection pressure required for the flowing porosity to reach 3.1% shows a relatively negative correlation with RQI (Figure 8c), the injection pressure here is in a reducing tendency while the RQI increases.

According to this study, the cutoff of effective porosity can be determined by the flowing porosity, the relationship between the effective and the flowing is listed in Figure 9. The low limit of flowing porosity here is 3.1%, so the effective porosity cutoff is given to be 4.0%.

Based on the above study, an effective discriminant chart of tight oil in the carbonate reservoir of interval MBK is established (Figure 10). The two red curves represent two different types of reservoirs. When the flowing porosity is greater than 3.1% and the injection pressure is greater than 19.9 Psi under reservoir conditions, the tight oil can accumulate and flow effectively. In the case of reservoir pressure is less than 19.9 Psi, the tight oil in type A samples cannot aggregate and flow effectively. The tight oil in samples of type B can't accumulate effectively because the flowing porosity is lower than the cutoff, even if the pressure under reservoir conditions is high enough.

Case Study

Well S-4-1 was tested in the MBK layer with section of 2262 m-2291 m, shown in Figure 11. From well log interpretation, it showed that the effective porosity was in the range of 1.0%-6.7% of this section, and the porosity in the range of 1.0%-4.5% occupied about 86.3%. According to the predecessor's study, the low limit of the effective porosity of the reservoir was 4.5%, and no oil test had been taken before. After this study, it was suggested to test the oil in the section, and the industrial oil flow which was about 37 m^3/d was obtained with 5 mm chock.

Conclusions

The flowing porosity under different mercury pressures can be obtained accurately by the high-pressure mercury injection experiment. According to the actual geological conditions in the block, the capillary pressure under reservoir conditions can be gained from the capillary pressure by mercury intrusion experiments, it can be used to calculate the flowing porosity under different reservoir injection pressures.

The injection pressure, the pore-throat ratio, the reservoir quality index (RQI) and the ratio of minimum pore-throat radius and 50% probability of pore-throat radius (RMP) have significant control over the flowing porosity of the reservoir. The pore-throat ratio and RMP affect the micro-mobility of the reservoir. With the increase of RQI, the injection pressure required to reach 3.1% of the flowing porosity is in a decreasing trend.
By studying and determining the flowing porosity of the oil-bearing and oil-free samples, 3.1% is chosen as the low limit of flowing porosity, 4.0% is the cutoff for the effective porosity, and the injection pressure is 19.9 Psi as the cutoff under reservoir conditions, so the tight oil above this injection pressure can flow and accumulate effectively. On the basis of the cutoff value of complex carbonate of the flowing porosity and injection pressure under reservoir conditions, the discriminant chart of effective accumulation of tight oil in complex carbonate of interval MBK in this block is established.

Acknowledgement

The authors would like to thank the "Global oil and gas resources assessment and constituencies with research" for support of this study; the fund numbers are 2016ZX05029 and 2017ZX05030.

References Cited

Anderson, W.G., 1987, Wettability literature survey: Journal of Petroleum Technology, v. 39/11, p. 1453-1468.

Feng, Minggang, Li Yan, Xueling Wang, et al., 2012, Lower limit for physical property of effective reservoir in Changxing Formation, Yuanba Gas Field: Petroleum Geology & Experiment, v. 34/5, p. 535-538.

Gong, Yanjie, Shaobo Liu, Rukai Zhu, et a1., 2015, Low limit of tight oil flowing porosity: Application of high-pressure mercury intrusion in the fourth Member of Cretaceous Quantou Formation in southern Songliao Basin, NE China: Petroleum Exploration and Development, v. 42/5, p. 681-688.

Harbaugh, J.W., 1967, Carbonate Reservoir Rocks, *in* G.V. Chilinger, et al., eds., Carbonate Rocks: Elsevier, Amsterdam, London, New York, p. 349-398.

Hu, Yong, Xinghe Yu, Gongyang Chen, et a1., 2012, Classification of the average capillary pressure function and its application in calculating fluid saturation: Petroleum Exploration and Development, v. 39/6, p. 733-738.

Li, Tong, Hekun Guo, Haibo Li, et al., 2013, Experimental research on movable fluid and NMR T2 cutoff in tight sandstone: Science Technology and Engineering, v. 13/3, p. 701-704.

Lucia, F.J., 2007, Carbonate reservoir characterization: Springer Verlag, Berlin, p. 29-83.

Mohammadlou, M.H., M.B. Mork, and H. Langeland, 2010, Integrated permeability analysis in tight and brecciated carbonate reservoir: SPE-131593, the SPE Annual Technical Conference and Exhibition in Florence, Italy, 19-22 September.

Rafatian, Navid, and Jon Capsan, 2015, Petrophysical characterization of the pore space in Permian Wolfcamp rocks: Petrophysics, v. 56/1, p. 45-57.

Rockwood, S.H., G.H. Lari, B.J. Langford, et al., 1957, Reservoir volumetric parameters defined by capillary pressure studies: AIME210, p. 252-259.

Standardization Administration of the People's Republic of China, 2008, GB/T 21650.1-2008 Pore size distribution and porosity of solid materials by mercury porosimetry and gas adsorption: Part 1: Mercury porosimetry: Standards Press of China, Beijing.

Yang, Shenglai, and Junzi Wei, 2006, Petroleum reservoir physics: Petroleum Industry Press, Beijing, p. 209-233.

Zhang, Hong, Shuichang Zhang, Shaobo Liu, et a1., 2014, A theoretical discussion and case study on the oil-charging throat threshold for tight reservoirs: Petroleum Exploration and Development, v. 41/3, p. 367-374.

Zhang, Yaowen, Qiang Chen, Junchang Dong, et al., 2014, Determination of the physical property lower limits of Z oilfield in the Middle East Area: World Well Logging Technology, v. 204/6, p. 30-44.

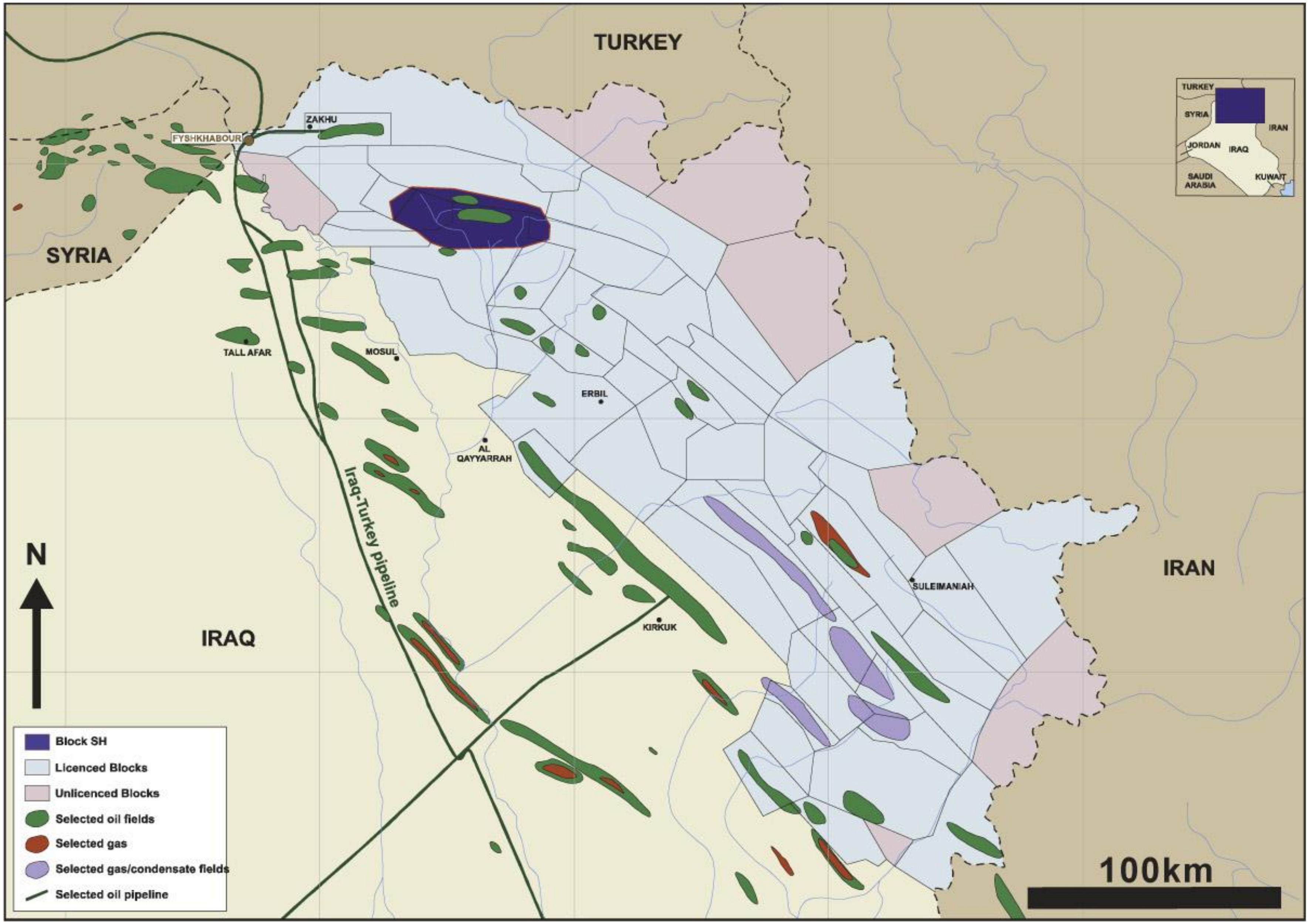

Figure 1. Location map of block SH.

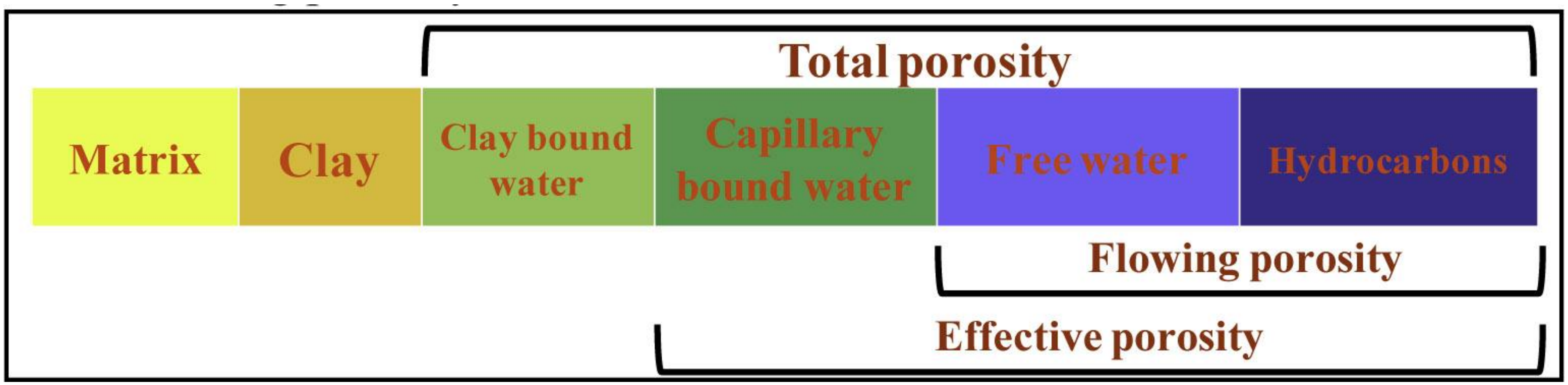

Figure 2. The porosity model in this study.

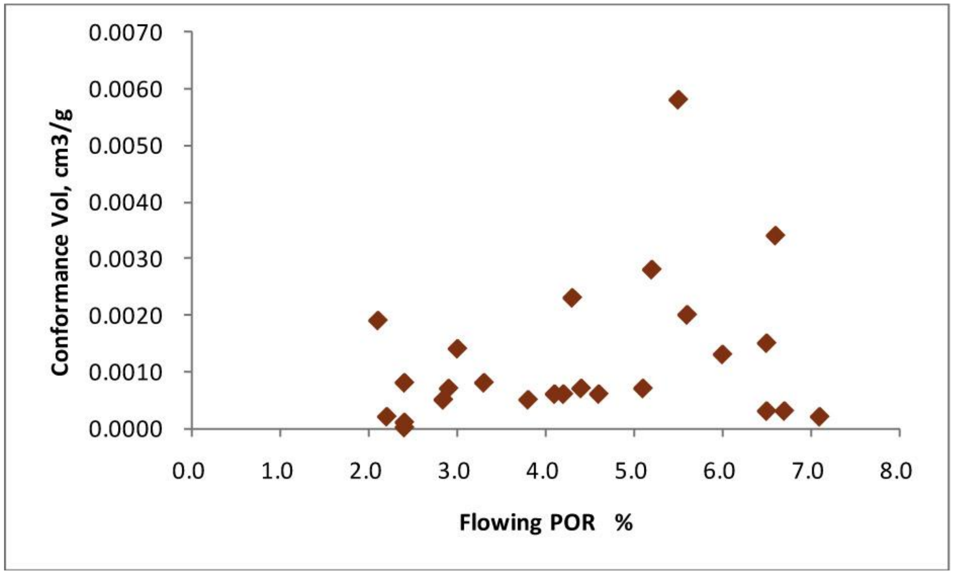

Figure 3.Cross-plot of CV and Flowing POR

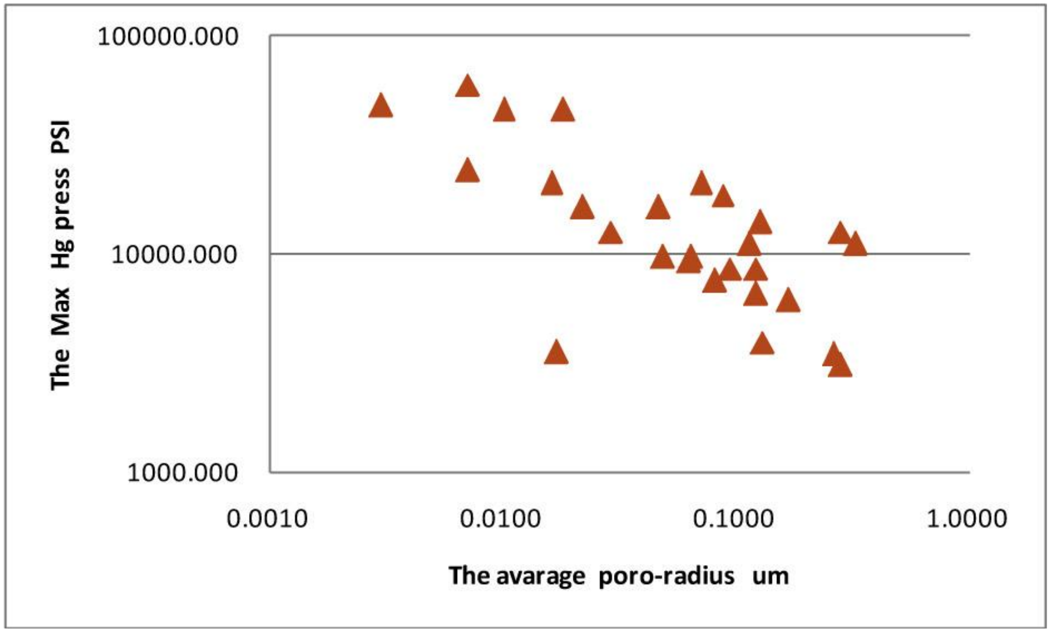

Figure 4. Cross-plot of Max Hg press and poro-radius.

Figure 5. Core photos of samples S65, S79 and S39.

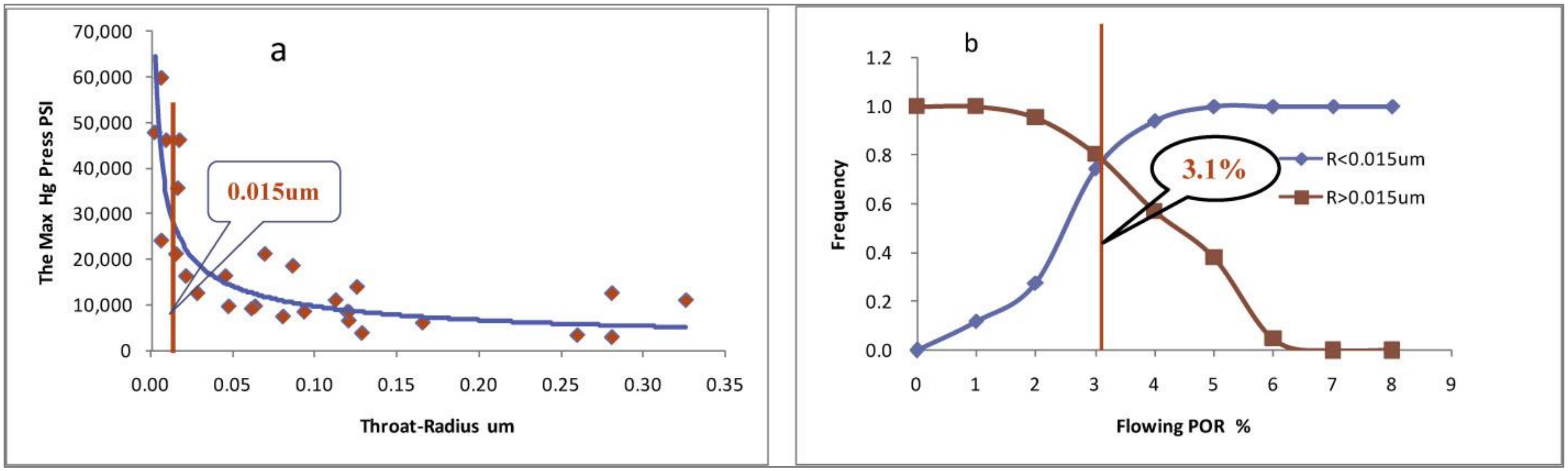

Figure 6. The plots to determine the cutoff of flowing porosity.

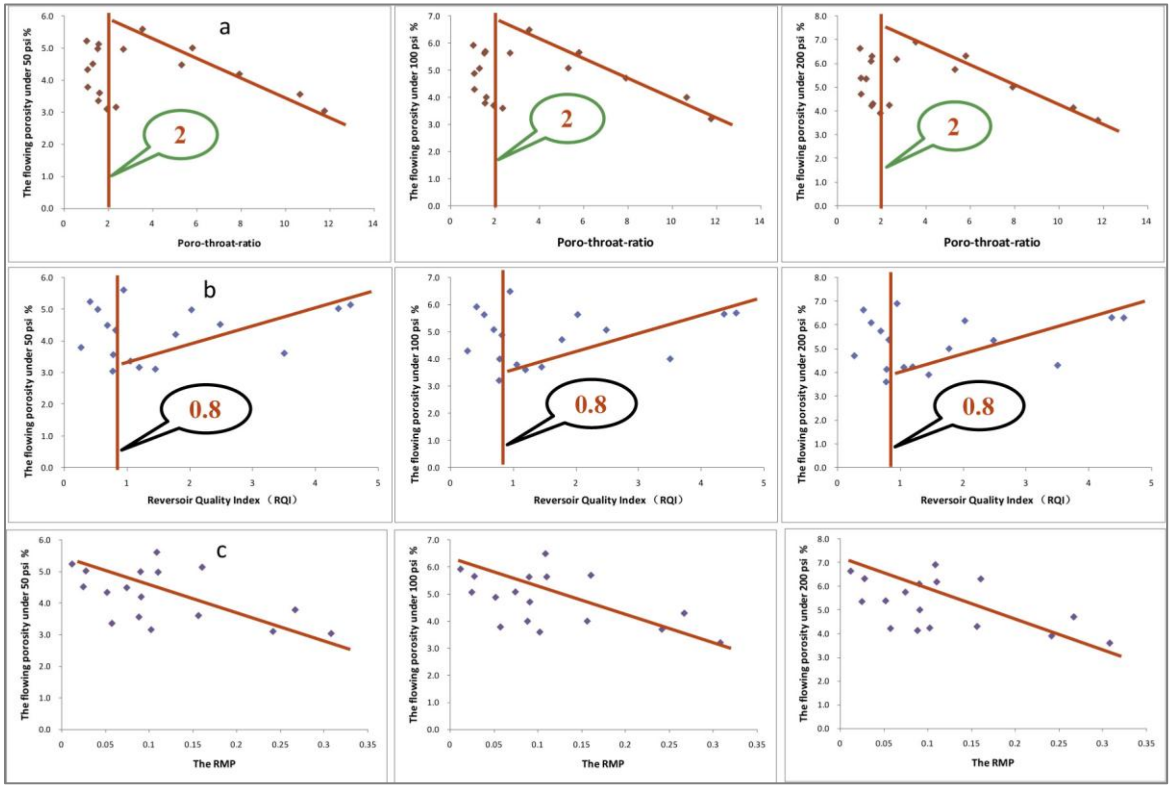

Figure 7. The controlling factors of the low limit, Flowing POR: (a) Poro-throat ratio, (b) RQI, and (c) RMP.

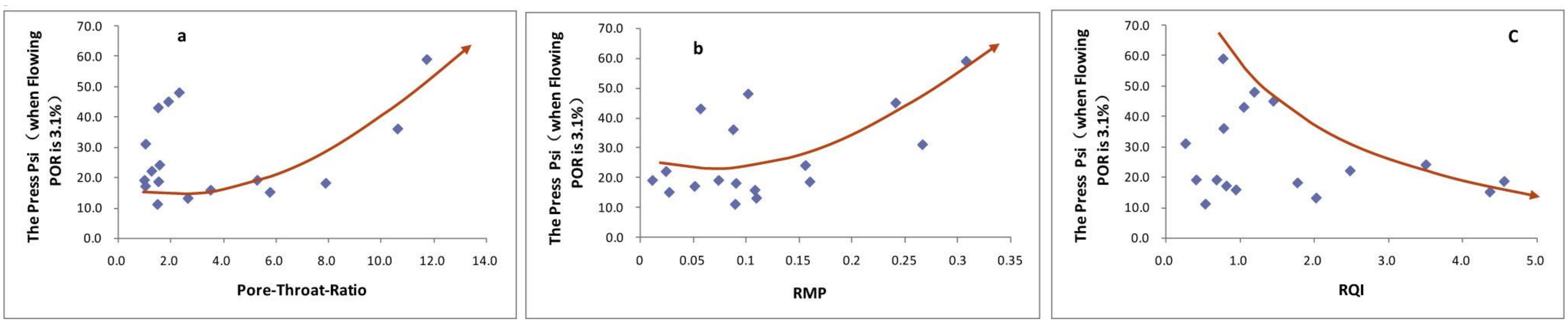

Figure 8. The tendency between press and pore-throat ratio, RMP, RQI.

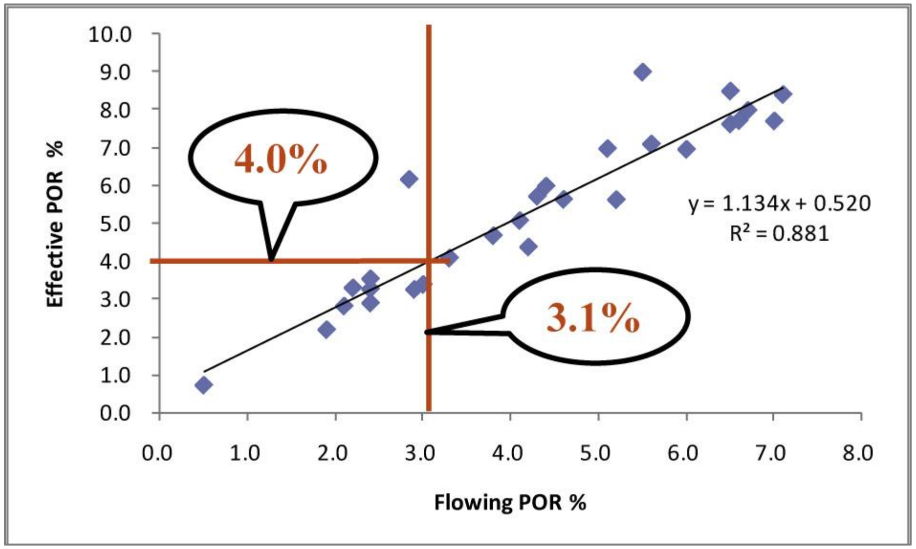

Figure 9. Relationship between effective and flowing porosity.

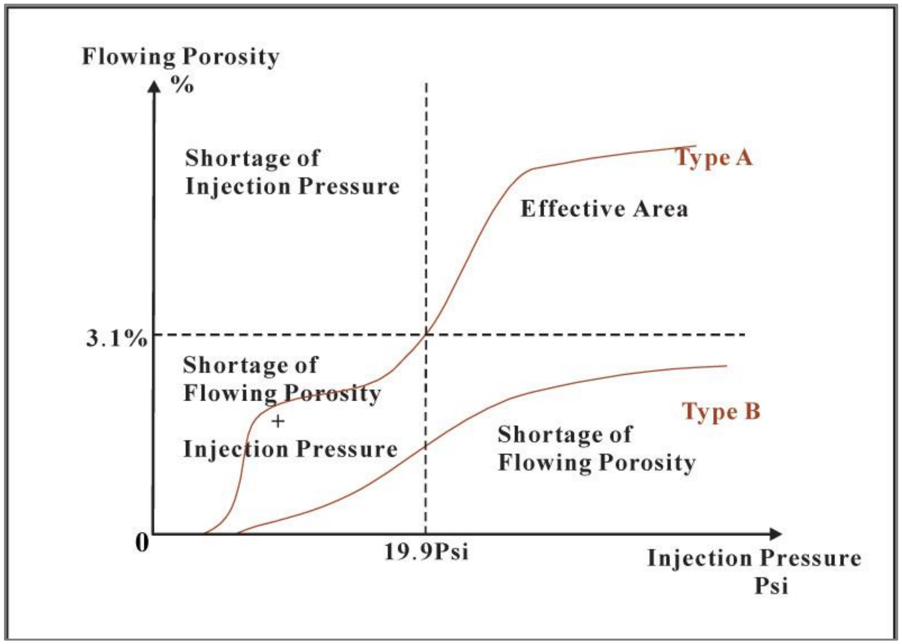

Figure 10. Discriminant chart of tight oil in MBK.

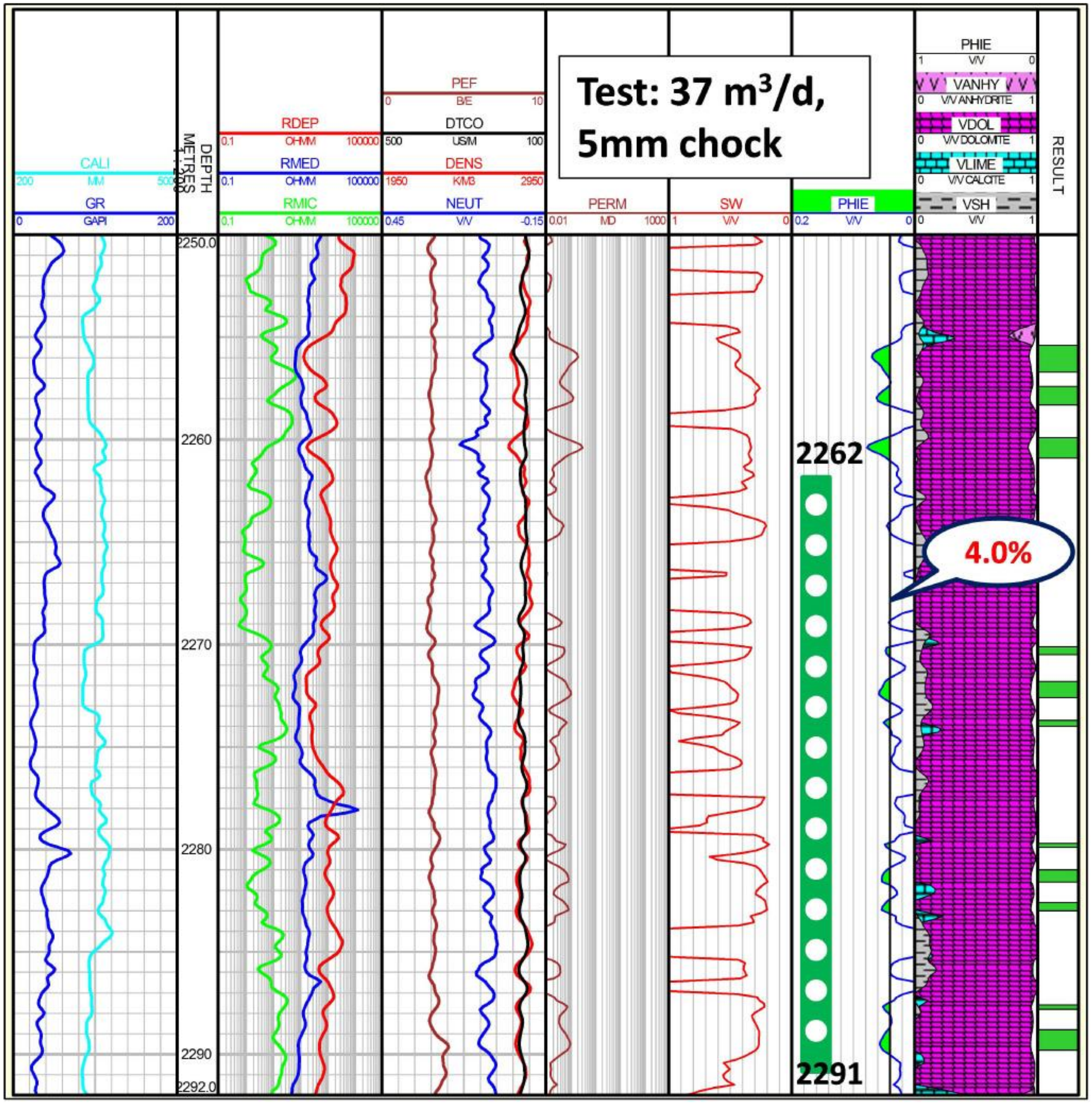

Figure 11. The plot of well S-4-1, 2250-2292 m.

Well	Sample	Depth m	POR_He %	POR_Hg %	Core Show	Oil or Not	Well	Sample	Depth m	POR_He %	POR_Hg %	Core Show	Oil or Not
S-1	S24	2249.50	6.9	6.0	Oil spot	Oil-bearing	S-6	S01	2278.09	0.7	0.5	No oil show	
S-1	S25	2250.79	9.0	5.5	Oil spot	Oil-bearing	S-6	S06	2279.06	7.7	7.0	Oil spot	Oil-bearing
S-1	S39	2255.42	8.0	6.7	Oil spot	Oil-bearing	S-6	S08	2280.08	2.2	1.9	No oil show	
S-1	S50	2262.98	3.4	3.0	Little fluorescence		S-6	S14	2281.04	6.0	4.4	Oil trace	Oil-bearing
S-1	S52	2267.42	3.2	2.9	Little fluorescence		S-6	S19	2281.63	8.5	6.5	Oil spot	Oil-bearing
S-1	S54	2270.78	7.0	5.1	Fluorescence	Oil-bearing	S-6	S26	2292.57	7.6	6.5	Oil spot	Oil-bearing
S-1	S62	2273.45	5.1	4.1	Fluorescence	Oil-bearing	S-6	S33	2296.33	5.6	4.6	Oil trace	Oil-bearing
S-1	S63	2276.43	7.7	6.6	Oil trace	Oil-bearing	S-6	S56	2297.05	4.4	4.2	Oil trace	Oil-bearing
S-1	S65	2280.17	4.1	3.3	Little fluorescence		S-6	S57	2301.06	3.3	2.2	No oil show	
S-1	S72	2282.82	6.1	2.8	No oil show		S-6	S60	2301.54	3.2	2.4	No oil show	
S-1	S74	2283.02	4.7	3.8	Oil trace	Oil-bearing	S-6	S61	2302.44	5.6	5.2	Oil trace	Oil-bearing
S-1	S75	2284.53	2.9	2.4	No oil show		S-6	S67	2303.77	5.7	4.3	Oil trace	Oil-bearing
S-1	S81	2285.09	2.8	2.1	No oil show		S-6	S68	2304.87	7.1	5.6	Oil trace	Oil-bearing
S-1	S83	2287.72	8.4	7.1	Oil spot	Oil-bearing	S-6	S79	2305.21	4.8	3.8	Little fluorescence	
							S-6	S86	2306.77	3.5	2.4	No oil show	

Table 1.The porosity of samples in this study block.

Sample	POR_He %	Flowing Por under different press %					
		Max Press	10 Psi	30 Psi	50 Psi	100 Psi	200 Psi
S14	6.0	4.4	0.5	2.0	3.2	3.6	4.2
S54	7.0	5.1	1.8	2.4	3.8	4.3	4.7
S56	4.4	4.2	1.5	2.3	3.6	4.0	4.1
S62	5.1	4.1	0.1	1.6	3.1	3.7	3.9
S67	5.7	4.3	1.5	2.6	3.4	3.8	4.2
S74	4.7	3.8	1.3	1.9	3.0	3.2	3.6
S06	7.7	7.0	1.4	3.8	5.2	5.9	6.6
S19	8.5	6.5	2.3	4.2	5.0	5.7	6.3
S24	6.9	6.0	2.1	3.3	4.5	5.1	5.7
S25	9.0	5.5	1.9	3.9	4.3	4.9	5.4
S26	7.6	6.5	2.3	4.6	5.0	5.6	6.1
S33	5.6	4.6	0.8	3.2	3.6	4.1	4.5
S39	8.0	6.7	2.3	4.2	5.0	5.6	6.2
S61	5.6	5.2	1.8	3.5	4.2	4.7	5.0
S63	7.7	6.6	1.8	3.5	5.1	5.7	6.3
S68	7.1	5.6	1.9	2.7	4.5	5.1	5.3
S83	8.4	7.1	1.7	4.1	5.6	6.5	6.9

Table 2. The 17 oil-bearing samples of MBK.

[Click to view slides of presentation.]